MODERN ELECTRONICS IN IMAGE-PROCESSING AND IN PHYSICAL MODELLING
- A NEW CHALLENGE FOR OPTICAL TECHNIQUES -

F. Mayinger

Lehrstuhl A für Thermodynamik, Technische Universität München, 80290 München, Germany

ABSTRACT

In heat and mass transfer and in fluiddynamics optical methods have a long tradition. For many years, however, processing data gained from optical techniques, especially from image-forming processes, was very time-consuming. New electronic devices and methods allow to reduce this data processing considerably and so image-forming processes like holography, holographic interferometry or Laser-Induced Fluorescence which provide comprehensive and detailed information on heat-, mass- or momentum exchange can be effectively and successfully applied to research and development in engineering. Modern data processing allows image-forming also from spotwise working optical techniques like from Raman-spectroscopy. A huge amount of data can be evaluated within a short time and can be composed to a clear, vivid but also meaningful information.

For describing complicated phenomena in fluiddynamics or in heat transfer by computer programs global experimental information is not sufficient. Optical techniques provide local and instant data without disturbing the process and with a high temporal resolution. By using the results of optical measuring techniques it is possible to improve computer programs describing physical processes, and optical techniques are also very sensitive touchstones for checking the quality and the reliability of such programs.

1. INTRODUCTION

Exactly 20 years ago - at the 5th International Heat Transfer Conference - the author (Mayinger and Panknin 1974) presented a paper on a new optical technique - the holography - which very newly came up during that time and offers great advantages for interferometric studies in heat- and mass transfer. Compared with the conventional interferometric techniques known before, the holographic interferometry offers many advantages to experimentalists. It is easy to handle, and the optical components are generally cheap to purchase. However, as with all optical methods the disadvantage existed that the data evaluation was very time-consuming and laborious. To evaluate an interferogram could take a full day work of a man.

Modern electronics together with newly developed computer software opened new prospects for holography and for holographic interferometry and not only for that, but also for other optical techniques by reducing the evaluation time down to minutes or even to seconds and by making it fully automatic just by using a personal computer. But also the electronics in the optical equipment itself got new dimensions.
Also other optical techniques which were principally known before, however, which were too complicated or too arduous for a meaningful quantitative data evaluation are now widely put into use again. Such new methods are, for example:

- light sheet photography and velocimetry,
- Laser-Induced Fluorescence ,
- Raman-scattering.

A more complete list of optical measuring techniques being of interest in heat and mass transfer and in fluiddynamics is given in Table 1.
This table also informs about the physical effect used by this optical measuring technique and gives application examples. Furthermore it tells the recording dimension - pointwise measurement or imaging method. Studying the possibilities of application in Table 1 one can see that parameters being of interest in heat and mass transfer - for example temperature, concentration, or velocity - can be investigated by various optical techniques. Velocity in a particle- or droplet-spray can be measured by pulsed laser-holography or by laser-doppler anemometry (LDA or PDA). For determining concentration fields Raman-scattering, Laser-Induced Fluorescence or holographic interferometry can be applied. Holographic interferograms

measuring technique	physical effect	application	dimensions	real-time application
schlieren and shadow	light deflection	heat, mass transfer	2d (integ.)	yes
holography	holography	particle size, velocity	3d	no
interferometry	change of light velocity	heat mass transfer	2d (integ.)	yes
laser Doppler velocimetry	Mie scattering	flow velocity	point	yes
dynamic light scattering	Raleigh scattering	density, temperature	point - 2d	yes
Raman scattering	Raman scattering	mol. concentration, temperature	point - 1d	no
laser induced flourescence	flourescence	concentration, temperature	point - 2d	no
absorption	absorption	concentration, temperature	point - 2d (integ.)	yes
pyrometry	thermal radiation	temperature	1d	yes
thermography	thermal radiation	temperature	2d (integ.)	yes
self flourescence	therm. flourescence, chemoluminescence	concentration, temperature	2d (integ.)	yes

Table 1: Overview of optical measuring methods

contain full information not only about boundary layers restricting transport processes, but also on local coefficients of heat and mass transfer. Laser-Induced-Fluorescence promotes a better understanding of combustion processes by conveying insights into the concentration- and the temperature-fields in and around a flame.

For describing complicated phenomena in fluiddynamics or in heat transfer by computer programs, global experimental information is not sufficient. Optical techniques provide local data without disturbing the process and with a high temporal resolution.

It is not possible to discuss here all optical techniques, which are of interest for heat and mass transfer and for processes - fluiddynamics, combustion - which are connected to it. Therefore a selection is made of optical methods with which the author has some experience.

2. HOLOGRAPHY

Holographic methods are in use since approximately 20 years, therefore, here only a few principles of that technique will be explained. Holography is an image-forming technique and can be applied for studying multi-phase fluiddynamic processes or together with interferometry to measure heat and mass transfer.

In Figure 1 the holographic two-step image-forming process of recording and reconstructing an arbitrary wave-front is illustrated. The object is illuminated by a monochromatic light source, and the reflected or scattered light falls directly onto a photographic plate. This object-wave usually has a very complicated wave-front. According to the principle of Huygens, one can, however, regard it to be the superposition of many elementary spherical waves. In order to simplify the matter, only one wave is drawn in Figure 1. A second wave called "reference-wave" is superimposed on the first one. If the waves are mutually coherent, they form a stable interference pattern, when they meet on the photographic plate. This system of fringes can be recorded on the photographic emulsion. The amplitude is recorded in the form of different contrast of the fringes and the phase in the spatial variations of the pattern.

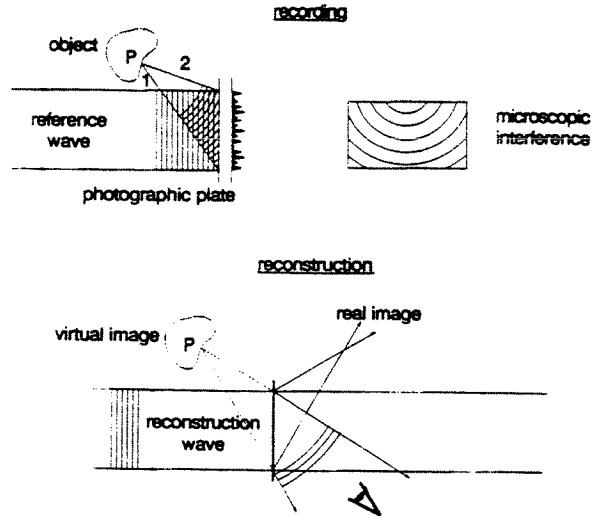

Fig. 1: Principle of holographic two-step image-forming process

If the plate, after chemical processing, is illuminated by a light beam similar to the original reference-wave, the microscopic pattern acts like a defraction grating with variable grating constant. The light transmitted consists of a zero-order wave, travelling in the direction of the reconstructing beam, plus two first-order waves. One of these first-order waves travels in the same direction as the original object-wave and has the same amplitude and phase distribution. This first-order wave produces a virtual image in the front of the holographic plate, seen from the side of the incoming reference beam. The other wave goes in the opposite direction and creates a real image of the object behind the photographic plate. This real image can be studied with various reconstruction devices, such as a microscope.

For conventional application of holography one can use lasers emitting continuous light, for which adjustment of the holographic plate is a trivial task. The recording of very fast moving or changing objects needs ultra-short exposure times, which can be achieved by using a pulsed laser, for example a ruby-laser with pulse durations of 20-30 ns. A holographic set-up using a pulsed laser is shown in Figure 2.

For adjusting such a holographic set-up with a pulsed laser one needs a second laser, emitting continuous

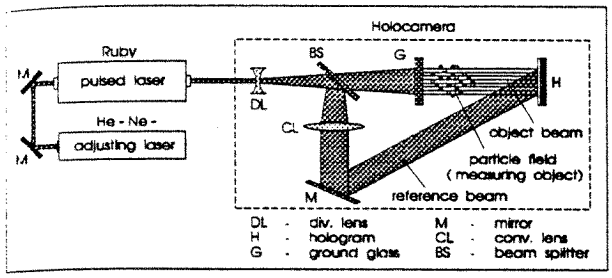

Fig. 2: Holographic set-up for ultra-short time exposures with a pulsed laser

light. With a ruby-laser as a light source one can use the special feature of the ruby crystal to transmit red light, which is emitted by a HeNe-laser.

A more sophisticated arrangement for recording pulsed laser holograms is shown in Figure 3.

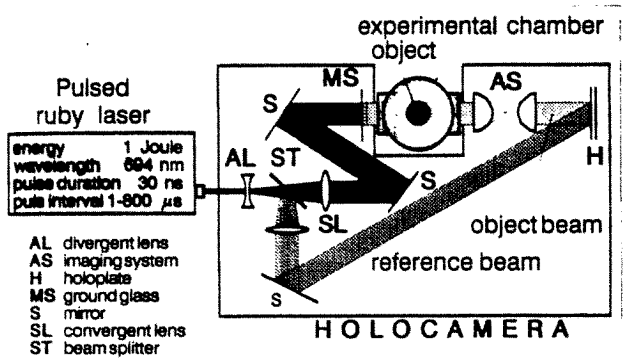

Fig. 3: Holographic interferometer for spray analysis

In this arrangement the light emitted by the pulsed ruby laser travels through a lens and a mirror system, where it is expanded, divided and guided through the measuring object and onto the holographic plate. This set-up is suitable for studying particle flow or phase distribution in multi-phase mixtures. It allows to visualize dispersed flow with particles or droplets not smaller than 10 λ where λ is the wave-length of the laser light.

If the electronic system of the ruby laser allows to emit more than one laser pulse within a very short period of time, sequences of the spray behaviour can be stored on the photograhic emulsion of the holographic plate, from which the velocity of the droplets as well as their changes in size and geometric form can be evaluated. The evaluation, however, needs a very sophisticated and computerised procedure. For evaluating the hologram, it first has to be reconstructed as demonstrated in Figure 4.

After chemical processing the holographic plate is replaced in the old position and then illuminated by a continuously light-emitting helium-neon laser.

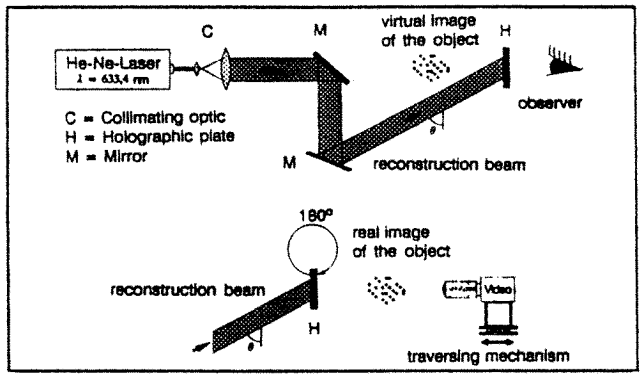

Fig. 4: Optical arrangement for the reconstruction of pulsed laser holograms

The new beam produced by this laser is now called a reconstruction beam. If the holograhic plate is replaced in the same orientation as during the recording process, one can look at it with the naked eye, and one sees a virtual image of the droplet spray exactly at the place where it was produced previously. For a quantitative evaluation one needs a closer examination via an enlarging lens or a microscope and by a camera preferably a video-camera. To do this the holograhic plate has to be turned by 180°, when positioning to the old place. By illuminating with the reconstruction beam a real image of the spray is now produced, which has a three-dimensional extension. The arrangement of the video-camera is shown in Figure 5. For technical evaluation the camera is moved forward or backward with a fixed focus of the lens, so that the spray cloud can be evaluated plane by plane.

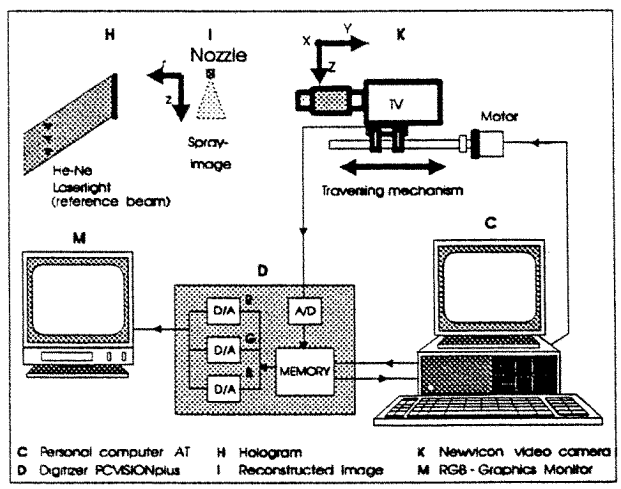

Fig. 5: Digital image-processing system for the evaluation of pulsed laser holograms

2.1 Computer-aided Evaluation

The very rapid development of computer technol-

ogy in the past decade as well as the miniaturisation and the mass production of computer chips made image analysis and image-processing applicable in many technical and scientific areas. Numerous problems of pattern-recognition, data handling of digitized pictures and computer graphics, formally only reserved for computing centres, can now be solved on a personal computer. The purpose of digital image-processing (DIP) is to reflect the main features of a picture more clearly and informatively than in the original and to judge the contents of an image quantitatively by employing pattern recognition algorithms. In the following the application of DIP for evaluating pictures of particle fields obtained from holographic reconstructions and the corresponding set-up of a PC-based image-processing system is briefly described.

Figure 6 shows schematically the basic steps, necessary to digitize a picture.

a) Superposition of a two-dimensional grid with a simple black and white image, to enable the spatial localisation of individual picture parts, a procedure which is called "Sampling" in TV technology.

b) Depending on the dominating colour in a grid box the casket in question is either coloured, black or white. This process is called quantization.

c) Transferring the pixel pattern into a binary matrix where 1 stands for the colour white and 0 for black.

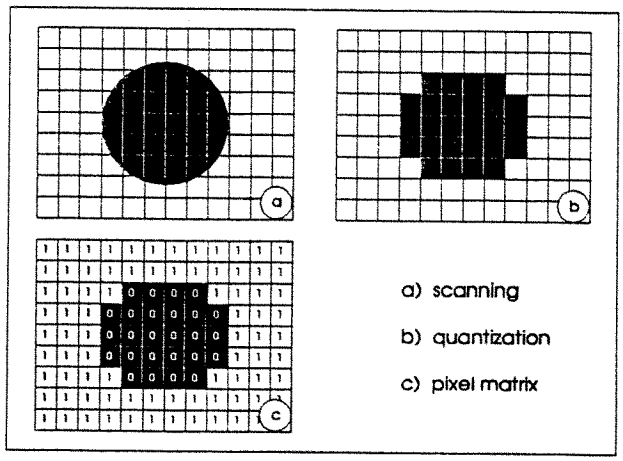

Fig. 6: The steps necessary to digitize a picture: Sampling and quantization

In contrast to black and white pictures, where the grid boxes can only take the value 1 or 0 grey pictures consist of various grey values. In a computer grey values are represented by bits; for the description of only two grey values one bit is sufficient. In byte orientated digitizers grey values are represented by one or two bytes. This provides a resolution of 256 colours in the case of one byte or 65 536 colours in the case of two bytes, each related to a grey value. As a convention the maximum grey value is associated with the colour white and the minimum with the colour black.

The quality of a digitized picture depends on the mode of digitization, i.e. on the sampling and on the quantization. Common grids for PC-digitizers vary between 512 × 480 up to 1024 × 1024 pixels with a depth of 1 byte for the grey value. For very high quality the width of a grid box should be of the magnitude of the grain of the photographic layer.
A detailed description of the numerical technique to perform the processes for grey value pictures can be found in Gonzáles and Wirtz (1977) and in Pavlides (1982). A good introduction was published by Haberäcker (1987).

If the pictures to be evaluated are obtained from holographic reconstructions by using a video-camera it is necessary to scan them. With the procedure of scanning we have to distinguish between in-line Holograms and off-axis Holograms. In the optical arrangement for recording in-line Holograms the optical axis of the object beam coincides with the reference beam. Both beams also coincide with the optical axis of the scanning camera. To resolve fine details of the object the scanning camera can be equipped with a micro-objective, which reveals only a small section of the whole picture. To scan the whole object part by part a relative movement between hologram and camera has to be facilitated. Equipments are on the market, which allow to fix a holographic plate in a traversing mechanism movable in three dimensions. The positioning of the plate-holder is realized by a piezo crystal, which works with a very high accuracy in the range of about 10 nm. A traversing mechanism which allows for movements of a larger distance and more or less in steps is shown in Figure 7.

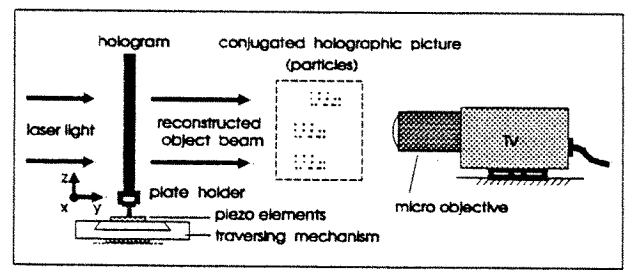

Fig. 7: Scanning of in-line-Holograms with a video-camera

For the reconstruction of off-axis Holograms a laser beam is used having the same angle of incidence at the holographic plate as the reference beam at the moment of the holographic record. The illumination of the holographic plate by the reconstruction beam

reproduces the object beam which contains the spatial information of the object. Also this holographic reconstruction can be scanned by a video-camera as before. In this case, however, the only possibility to realize the relative motion between reconstructed picture and video-camera is to move the video-camera. A movement of the photoplate would change the illumination.

An example for a digital image-processing system was already shown in Figure 5. This system is able to evaluate both in-line and off-axis holograms. In the following the processing of off-axis holograms will be briefly described. The hologram **H** is reconstructed by illuminating the photo-plate with a continuous, parallel beam of a HeNe-laser, which serves as a reference beam. The video-camera **K** scans the image of the holographic reconstruction **I** (for example the real image of a spray) and transmits the information to the digitizer **D**. There the signal is transformed from analog into digital and is stored in the digitizer frame memory. The processing of the digitized picture is then carried out by the computer, using the digitizer frame memory interactively for pixel allocation. In order to visualize the information actually stored in the digitizer frame memory, a continuous pseudo colour output signal is produced which can be observed on the graphics monitor **M**.

The video-camera can only record two-dimensional pictures in an octagonal plane to the axis of the lens, and so to get out the full information from the three-dimensional holographic image, this image has to be reproduced in and transformed into a series of many two-dimensional video pictures. This is done by moving the video-camera backwards and forwards with the help of the traversing mechanism. So, for example, the video-lens is focused to the mid-plane of the reconstructed holographic picture, and after processing these mid-plane data, the next plane could be evaluated by adjusting the focus of the lens in a proper way. This, however, would have the draw-back that the scale of this new plane would be different from the old one. Therefore, the camera is moved with fixed focus. The movement of the camera via the traversing mechanism can be controlled and monitored by the computer.

2.2 Filtering Operations, Image Identification and Focusing Criteria

The processing of images obtained from holograms involves: The separation of the image from the background, identification of sharp focused image parts, measuring of their projected areas and, for example, evaluation of their equivalent diameters or centre points with respect to a reference frame. These processing steps will be explained using the example of a dispersed two-phase flow behind an injecting nozzle. By applying an average filter, the noisy background can be suppressed or its frequency can be minimised. There is software on the market which can be used to do this. Therefore, it will not be explained in detail here.

After the suppression of the noisy background the sharply focused parts of the image - in this case droplets - have to be identified and clarified. This can be realised by contouring the parts of the image. To explain this procedure, instead of droplets in the spray more simple objects are chosen here, namely glass pearls adhered to a thin wire. Figure 8 presents two reproductions of a hologram taken from these glass pearls where the first one was well focused, and the second one was 1 mm out of focus. The histograms in Figure 8 represent the grey value along the line, which cuts the contour of the second pearl. From the observation of both images and their corresponding histograms it is obvious that sharply focused contours deliver a strong gradient of grey values, and unsharply focused ones show a smooth transition of the grey values. The decision about the sharpness of a contour is made by a digital image-processing system. For this procedure many so-called autofocus-algorithms have been developed and are available from the literature (Ligthart and Groen, 1982). Based on the different gradients of the grey values, a Sobel-operator enhances strong gradients while makes to disappear images with weak gradients. The last step is to eliminate all images, which are not well focused. This can be done by allowing only pixels to remain in the image, which have a grey gradient to their neighbours above a certain value. For details reference is made to the work by Chávez and Mayinger (1992). By this procedure a "picture" is electronically produced containing only contours, which are within a very narrow tolerance of the focusing plane.

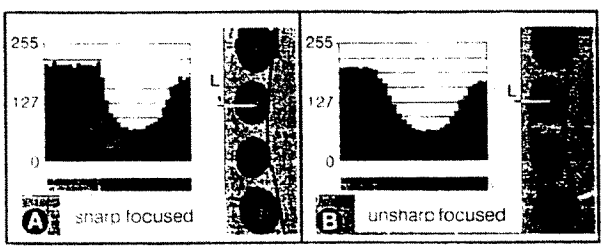

Fig. 8: Histogram of grey value of a sharply focused and an unsharply focussed image.

It may happen that the contours of some parts - for example droplets - do not have a closed and

continuous outline, because pixels may have been extinguished spotwise during the gradient checking procedure. Therefore, a next step has to follow in which the open contours are filled with colour to produce closed out lines of the particle reproduction. In order not to create new spots by this process, the situation after the contouring is compared with that, which existed before the out-off-focus particles were eliminated. A "particle" in the new picture is only accepted, if it existed already in the original picture. Finally the remaining particle reproductions are filled with colour, and now the evaluation with respect to particle size, form and concentration can go on.

An example of a computerised reproduction of the veil and the droplet swarm originating from a nozzle is shown in the Figures 9 and 10 (Chávez and Mayinger, 1990 and 1992).

They convey an impression of how the information of a hologram can be improved by computerised

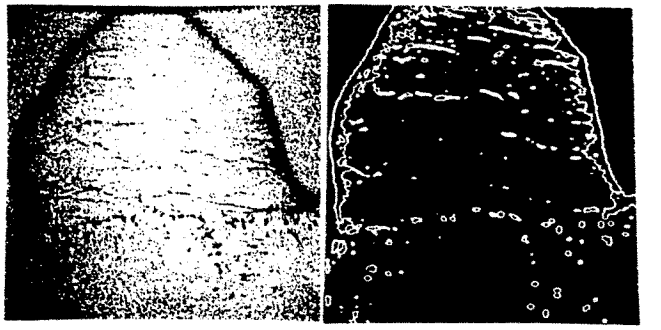

Fig. 9: Veil and spray flow behind a nozzle: Photographic view and evaluation of the hologram

evaluation. While the photograph on the left-hand side of Figure 9 shows only the shape of the veil, the computerised picture on the right-hand side clearly presents the thickness of the liquid film of the veil and also shows its wavy nature. In addition the droplets separating from the lower end of the veil are

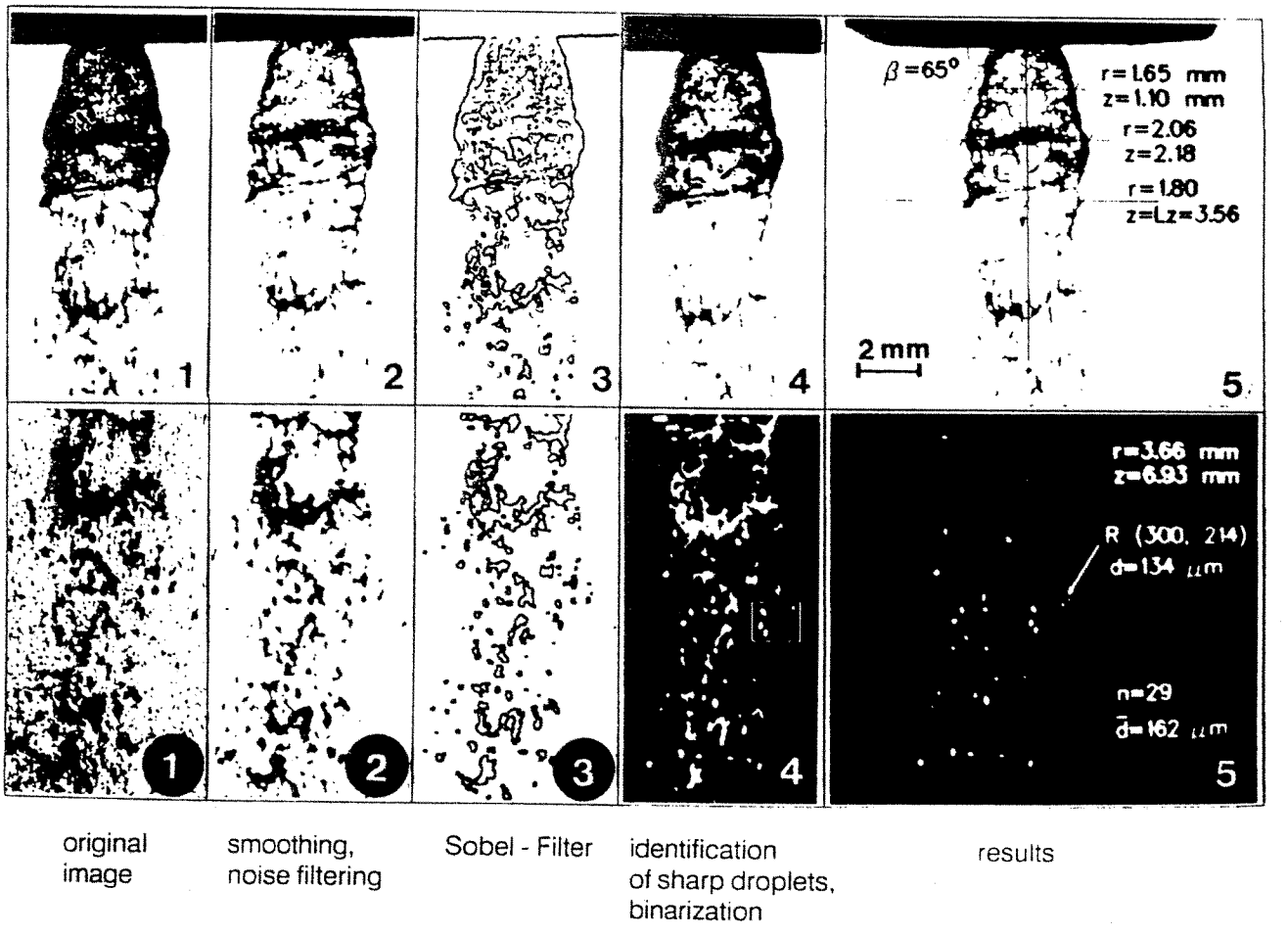

Fig. 10: Steps of image-processing of a hologram. Upper row: spray near the nozzle. Lower row: Spray downstream the nozzle.

clearly defined. Figure 10 presents the sequence of reproduced "pictures" by this computer-aided image-processing. The upper row in this figure shows the region of the spray near the nozzle, and the lower one a region further downstream, where the veil already is disintegrated into a droplet swarm. By applying specially developed algorithms (Chávez 1991), the cross section area, the diameter and the concentration of the droplets can be determined. The figure gives an impression how the numerical procedure changes the original photographic picture into a computerised one, which contains only information of particles, being exactly in the focus plane, a slice, which is thinner than 0,5 mm.

2.3 Double Exposure Technique

If two exposures of a moving particle collective are illuminated onto the same holograhic plate within a short time, the velocity of the particles can be determined from such a hologram (Chávez and Mayinger 1992). To evaluate such a double-exposed hologram, first the same procedure has to be performed as briefly discussed before. After that the centre point of each particle has to be defined by the computer, which is the basis for determining the distance between the two images of the same particle and for evaluating the velocities and trajectories of the particles. This method again is explained with the example of a moving droplet swarm. At first it is assumed that the particles are only moving in a two-dimensional way, i.e. within the focused layer of the hologram reproduction. To make the task easier, the criterion for distinguishing between well-focused droplets and droplets out of focus is reduced, i.e. also images of droplets with little less steep gradients are regarded as if they would move in the well focused plane. By this also droplets which not exactly are moving in the well-focused plane can be taken in account.

In the next step the computer starts a process in which each image of a droplet is connected with all other ones, and where the distance as well as the angle with reference to the nozzle axis between two "images" is determined. Now a Fourier analysis is applied, which converts the spatial distribution into an normalised frequency distribution as shown in Figure 11 for the angle of the connecting lines. The preferential angle appears as a peak in the Fourier diagram, showing the main direction and by this the direction of the movement of the particles. In the next step the same is done with the distance of the droplet "portrait". Now the preferential distance appears as a peak in the Fourier diagram, from which the mean velocity can be calculated by using the time distance between the two exposures.

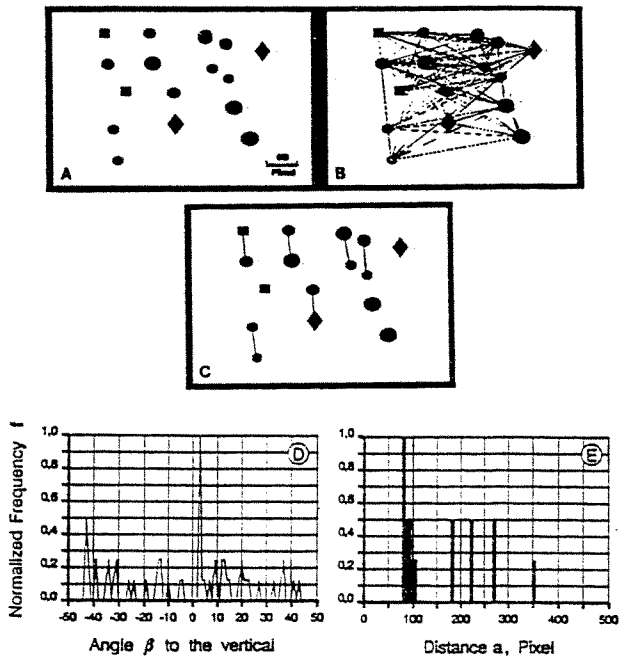

Fig. 11: Steps for the recognition of couples of spots corresponding to two successive positions of droplets.

If one is also interested in the velocity distribution of the droplets, a further procedure has to be performed. Now the computer defines a searching area in a spatial distance from each particle, portrayed with the information of the mean distance, gained from the procedure done before. This definition of the searching area is illustrated in Figure 12. Then the computer is searching for an image of a particle in this area, and if it finds one there it defines it as the second exposure of the particle at position 1. Then the real velocity and the direction of the droplet can be calculated. If the computer does not find a particle image within this searching area, it cancels the input of position 1 for this first step of the calculation but stores it for a next step where focus plan in front or behind this first plane is processed, assuming that the particle moved out of the focused plane before the second exposure was done.

If the movement of the particles is strongly three-dimensional, the procedure is much more complicated. In such a case electronically reproduced pictures of 3 or more focus planes have to be taken in account, and the searching for the image of the second exposure of a particle has to be extended to all these planes being under consideration. So the Fourier analysis can be made in a three-dimensional way.

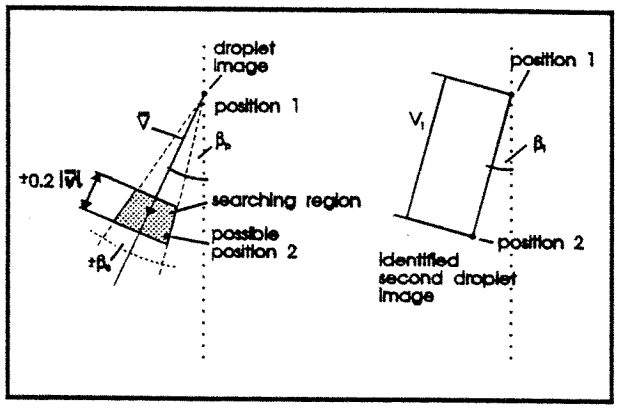

Fig. 12: Method for evaluating particle velocity from double pulsed holograms

The data produced by this opto-electronic process are of high accuracy as Figure 13 demonstrates. The method is so accurate that even the influence of the pressure of the atmosphere, in which the droplets are travelling, can be clearly brought out. Of course, the mass flowrate through the nozzle has a great influence onto the droplet velocity as demonstrated in Figure 13, which presents the average droplet velocity after disintegration of the veil.

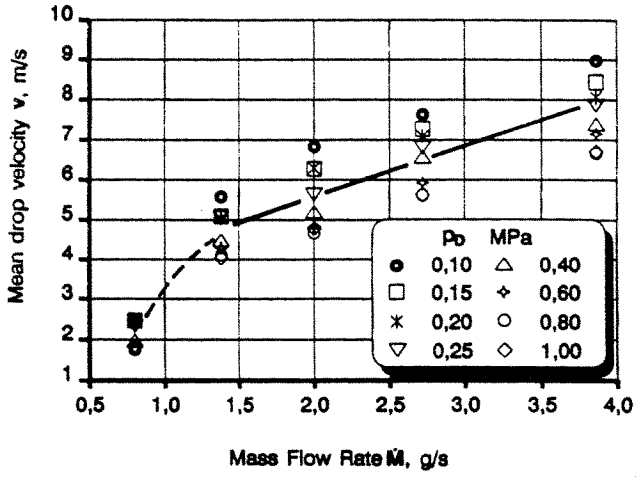

Fig. 13: Mean droplet velocity in a spray as a function of the flow-rate at different ambient pressures

3. INTERFEROMETRY

By using the recording capabilities of holography different waves - even those shifted in time - can be stored in the same holographic plate. If the developed holographic plate is illuminated with the reference wave, all objects waves are reconstructed simultaneously. Where they differ only slightly from each, other interference pattern are observed. These are the fundamentals of holographic interferometry.

In heat and mass transfer the temperature and the concentration distribution in a fluid are of special interest. To investigate processes with heat and mass transfer a so-called through light method is used where the object wave is irradiating through a volume, in which the transport processes take place. An exemplary arrangement for holographic investigations is shown in Figure 14. A beam splitter divides the laser-beam into an object wave and into a reference wave, which is also called comparison wave. Both waves are expanded to parallel wave bundles behind the beam splitter via lenses, usually consisting of an arrangement of a microscopic lens and a collecting lens. The expanded and parallel organised object wave travels through the space, with the research object of interest - the test-section - and in which the distribution of temperature or concentration is of interest. The reference wave bypasses the test-section and falls directly onto the photographic plate.

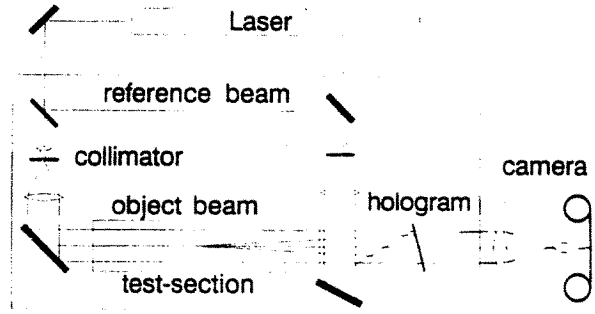

Fig. 14: Optical set-up for holographic interferometry

The benefit of holographic interferometry compared to other interferometric methods - like Mach-Zehnder interferometry - is that there is no need for a high optical quality of the optical components, because only relative changes of the object wave are recorded, and optical errors are automatically compensated by the interferometric method. On the other hand, the monochromatic light producing the wave-front has to be very stable, therefore, a laser of good coherency is needed as light-source. There are many possibilities for arranging the optical set-ups to form a holographic interferometer, which cannot be discussed here in detail. Reference is, therefore, made to the literature (Mayinger 1991, Mayinger and Panknin 1974, and Panknin 1977).

Several procedures exist to produce interferograms; here only one method will be explained, which can also be used in connection with high-speed cinematography. It is called the "real-time method", because it observes the process to be investigated in

real-time and continuously. The method is illustrated in Figure 15. After the first exposure by which the comparison wave is recorded and during which no heat transfer is going on in the test-section, the hologram is developed and fixed. Remaining at its place or repositioned accurately, the comparison wave is reconstructed continuously by illuminating the hologram with the reference wave. This reconstructed wave showing the situation without heat transfer in the test-section can now be superimposed onto the momentary object wave. If the object wave is not changed compared to the situation before the chemical developing process and if the hologram is precisely repositioned, no interference fringes will be seen on the hologram.

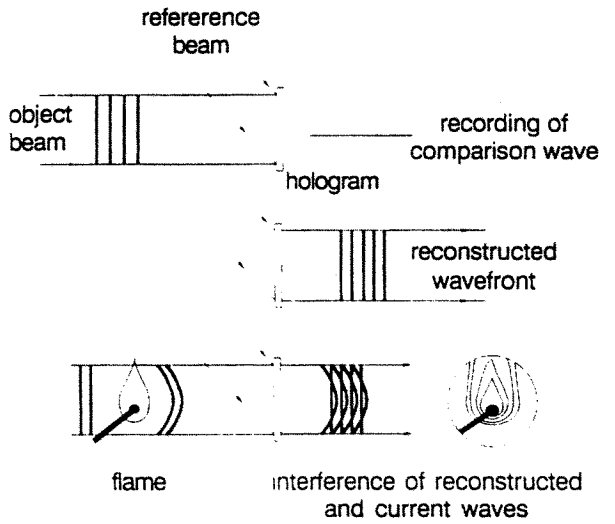

Fig. 15: Real-time method for holographic interferometry

Now the heat transfer process can be started. Due to the heat transport a temperature field is formed in the fluid, and the object wave receives an additional phase-shift, when passing through this temperature field. Behind the hologram both waves interfere with each other, and the changes of the interference pattern can be continuously observed or photographed.

An example of an holographic interferogram taken with this method is illustrated in Figure 16 where the temperature- and heat transfer-distribution around 3 tubes in a bundle with longitudinal flow is demonstrated. The tubes are in a staggered arrangement. Each black and white line in this interferogram represents a zone of constant temperature according to the optical laws of interferometry, which will not be explained here, but which are discussed in detail in the literature, for example, by Hauff and Grigull (1970) or by Mayinger (1991). Because the heat transport density is proportional to the temperature gradient in the boundary layer, the interferogram in Figure 16 immediately tells where local zones of high heat transport exist, namely there where the interference fringes and by this the isotherms have a small spatial distance. This is generally the case at the narrowest gaps between 2 tubes. Plotting the temperature gradient versus the distance from the heated wall by using the interference pattern and extrapolating this plot to the wall surface, one gets the temperature gradient directly at the wall. This gradient times the thermal conductivity is equal to the heat transfer coefficient times the temperature difference between wall and bulk. So the heat transfer coefficient can be evaluated without knowing the local heat flux, just by using the information from the interference pattern and by measuring one temperature with a thermocouple either the wall- or the bulk temperature.

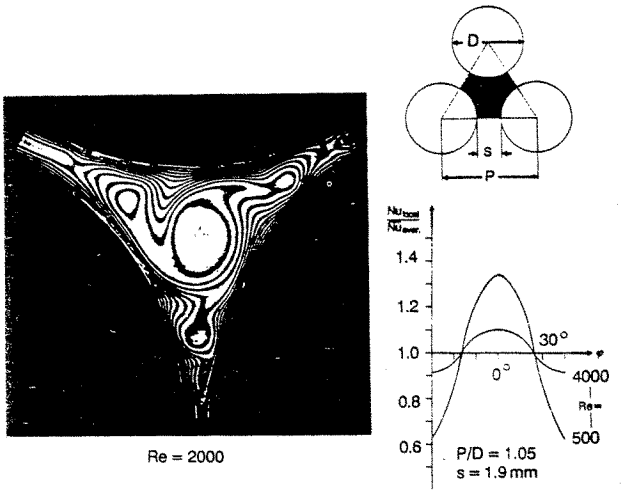

Fig. 16: Temperature field between three heated tubes with coaxial flow

Not only two-dimensional temperature fields can be measured by holographic interferometry but also three-dimensional ones, for example, spherical and cylindrical temperature fields. In these cases the Abel correction has to be used, which is described by Hauff and Grigull (1970) or by Chen (1985).

3.1 Evaluation of Holographic Interferograms

Evaluating a holographic interferogram by hand as it was done for long years until short time ago, is a very time-consuming and tedious task. Today also for this procedure computerised evaluation is available, which reduces the time needed for deducing the local Nusselt-numbers out of an interferogram from several hours down to a few seconds. For computerised eval-

uation one needs the same components as described before, namely a video-camera, a digitizer, a graphic monitor and a personal computer. In the first step the procedure is very similar to that explained in section 2. New is, however, that the distances of the interference lines near to the wall have to be determined very exactly, and this presupposes that the positions of the maxima of the darkness within these interference fringes are precisely known. To find the maximum of greyness or darkness, similar algorithms can be used as described in chapter 2, and histograms of grey value can be developed, now however, not for distinguishing well focused particles from out-off focus ones but for finding the maximum of greyness. The procedure will be published more in detail in Mayinger (1994).

Before determining the spot or line of maximum greyness orthogonals have to be drawn from the surface of the wall, because heat is transported normally to the wall, and the isotherms are running orthogonal to the direction of heat transport. Therefore, at first the contour of the heat transferring wall has to be formulated in a digital way on the computer. The surface points of the wall as represented in the interferogram can be interactively marked by using a mouse. Storing these surface points in the computer one has to distinguish between points only describing the perimeter (perimeter points) and points where the heat or mass transfer has to be calculated (evaluation points). The perimeter points serve only to describe the surface, and the knowledge of their position is only necessary at corners with a non-continuous curvature, for example. The distinction between perimeter points and evaluation points is made by using a "flag", which is set to zero for perimeter points and to 1 for evaluation points. The coordinates of each point including the flag are stored in a file on the hard drive and can be applied for the examination of any interferogram around one and the same wall contour. The number of points influences the evaluation accuracy, of course.

In the next step the perpendicular to the wall surface has to be found. To do this a circular segment is drawn through the evaluation point P and through two neighbouring points A and B as shown in Figure 17. From this circle the perpendicular at point P can be determined.

Finally the distances between 2 extremas of greyness along this perpendicular has to be expressed in numbers of pixels and then converted into metrical units. The conversion factor can be calculated from corner points in the interferogram, which are parts of the contour of the heat transferring wall and the

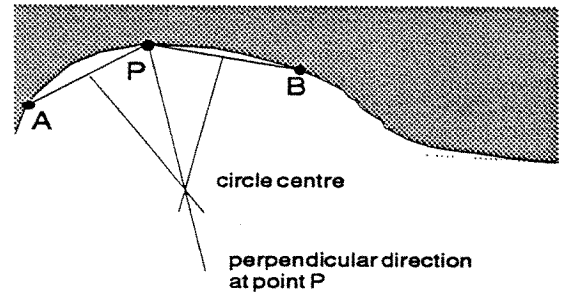

Fig. 17: Determination of the perpendicular direction at the evaluation point P

distance of which is known. Finally the heat transfer coefficients and from these the Nusselt-numbers can be calculated with high local and temporal resolution.

With very high heat transfer coefficients the boundary layer at a heat transferring surface becomes very thin down to a few hundreds of a millimeter. In this case it is difficult to evaluate the interference pattern if it is registered with the procedure described up to now. A slightly altered method, the so-called "finite fringe method" offers some benefits. In this method after the reference hologram was produced a pattern of parallel interference fringes is created by tilting the mirror in the reference wave of Figure 18, or by moving the holographic plate there within a few wavelengths. The direction of the pattern can be selected

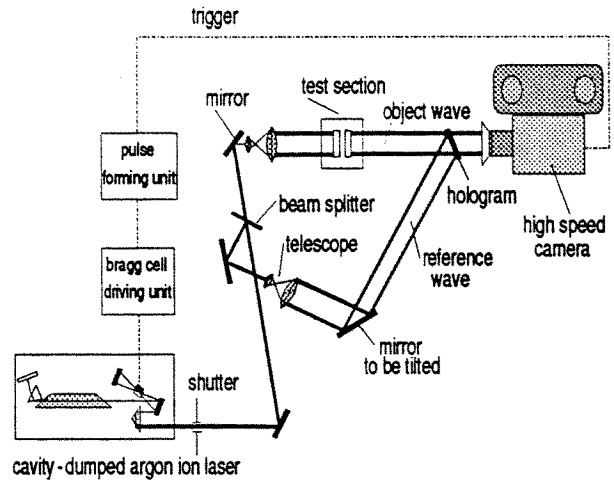

Fig. 18: Finite fringe method for holographic interferometry

as one likes, and it is only depending on the direction of the movement of the mirror or of the holographic plate. This pattern of the parallel interference fringes is then distorted by the temperature field due to the heat transport process. The distortion or deflection

of each fringe from its original parallel direction is a measure for the temperature gradient at this spot and allows to deduce the heat flux and by this the heat transfer coefficient.

Figure 19 demonstrates the possibilities of using these techniques in a flow with a bubble condensing in a liquid. By combining this method with high-speed cinematography it allows an inertialess and precise evaluation of the heat transfer coefficient at the phase-interface of the condensing bubble.

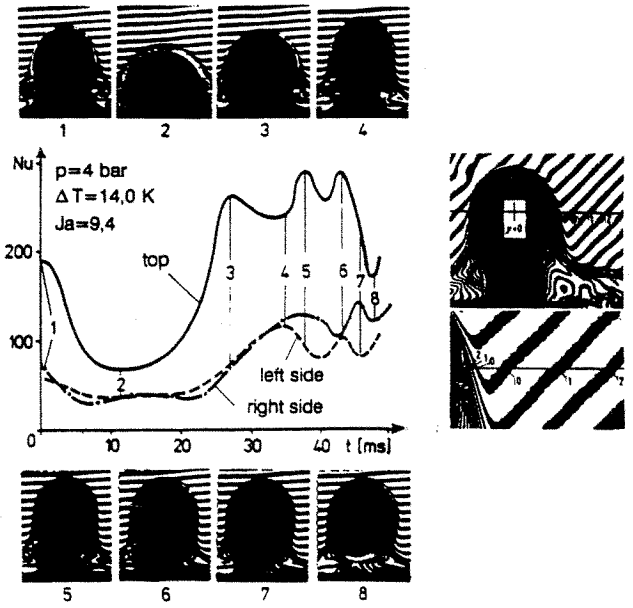

Fig. 19: Heat transfer at the phase-interface of a vapor bubble condensing in a subcooled liquid, deduced from a sequence of interferograms

3.2 Two-Wave-Lengths Method

The phase-shift of the light-wave when travelling through a gas or liquid is a function of the change in the density of the fluid. In multi-component systems the temperature and the concentration can influence the density. Interferometry usually works on the assumption that the alteration of the density is effected by a temperature change only. If variations in the refractive index are caused additionally by concentration, i.e. if two unknown variables, the temperature and the concentration influence the interference pattern, one needs an additional information to solve the interferometric equations. This can be done by using a second laser, emitting light of different wavelengths than the first one since the refractive index is depending on the wave-length of the light as known to everybody by the rainbow phenomenon. So 2 sets of equations are available - for each wave-length one - and the system is solvable for 2 unknown variables.

The two-wave-lengths interferometry was first proposed by El-Wakil et.al. (1966) for Mach-Zehnder interferometry and was very successfully developed by Panknin (1977) and by Panknin and Mayinger (1978) for the holographic interferometry. The problem with this two-wave-lengths interferometry is, however, that the two interferograms originating from these two beams of different wave-lengths have to be superimposed very accurately. Here the peculiarity of the holography allowing the recording of different interference pattern on one and the same plate is a great help to overcome these difficulties. A simple set-up for the holographic two-wave lengths interferometry is shown in Figure 20. It resembles very much the arrangement of Figure 14 and actually the only difference is that two lasers are used as light sources, a HeNe-laser, emitting red light and an argon-laser, emitting green light. The two beams intersect and at the position of this intersection a shutter is placed, which guarantees equal exposure times for both waves. The beams are then superimposed by means of a beam splitter which results in two object and two reference-waves at different wavelengths. For the evaluation of these two superimposed interferograms, reference is made to the thesis by Panknin (1977).

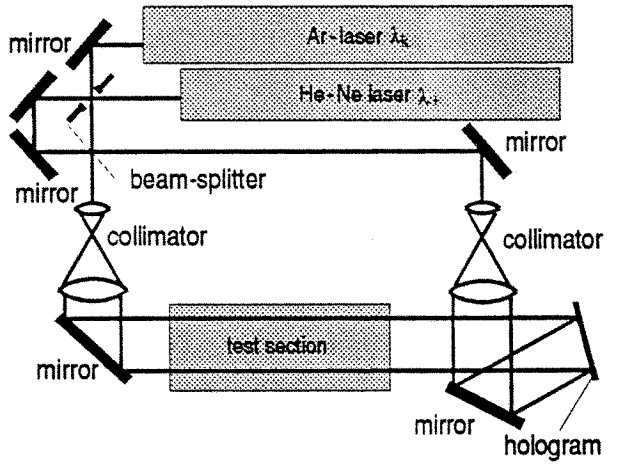

Fig. 20: Optical set-up for holographic two-wavelength interferometry

A simple example for an application of the two-wavelengths technique is shown in Figure 21. A horizontal cylinder was paved with naphtalene and heated from inside. The heat and mass transfer were generated by a natural convective upward air-flow. From the interference pattern the Nusselt- and the Sherwood-numbers were determined. Since air was the cooling and absorbing fluid having a Prandtl- and a Schmidt-number near to 1 the circumferential distributions of the Nusselt- and the Sherwood-number look very similar.

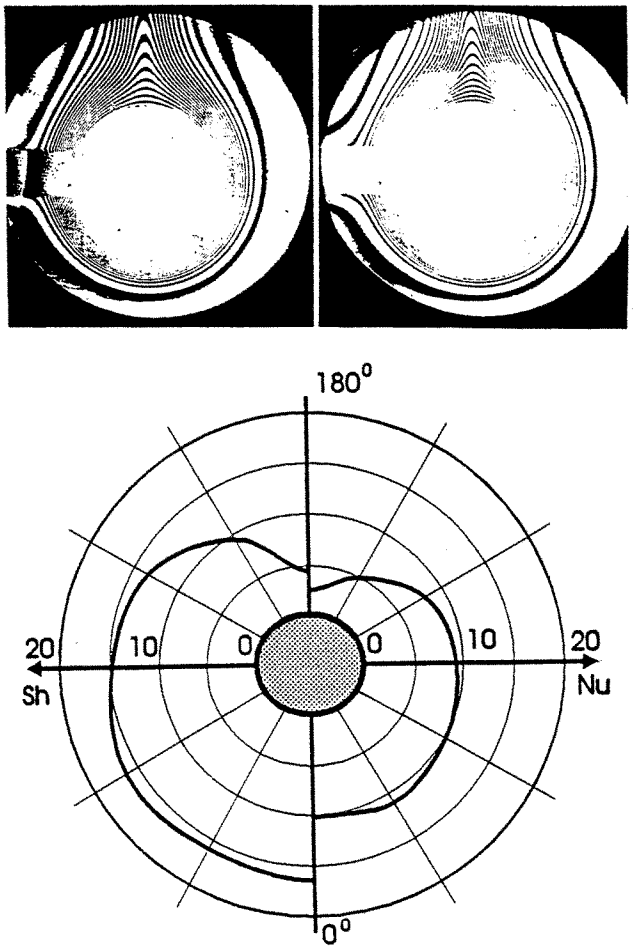

Fig. 21: Two-wavelength interferogram of combined heat- and mass tranfer during free convection around a cylinder evaporating Naphtalene

4. LIGHT SCATTERING METHODS

Light as sensor can provide several information and not only the refractive index and the phase-shift can be used to get information about the distribution of concentration or temperature in a substance. Besides the phase-shift the effect of scattering is most commonly used to get information about the chemical and physical conditions in a gas or a liquid. Raman-scattering is a method, which allows to measure the variety of substances present in a mixture, the concentration of each species and under certain circumstances also the temperature. Rayleigh-scattering can be used as a non-intrusive method for measuring the temperature. The fluorescence indicates the kind and the density of atoms and molecules and also allows to deduce the temperature. There are also other scattering methods like Mie-scattering used in Phase-Doppler-Velocimetry, Bragg-scattering for detecting density fluctuations and for investigating the structure of crystals and Brillouin-scattering for measuring sound velocity and sound absorption. Here only the fluorescence used together with a light sheet method and the Raman-scattering will be discussed.

It should be briefly mentioned that Mie-scattering is recently used for flow visualization in the particle image velocimetry (PIV). A laser beam is formed into a very thin light-sheet illuminating a plane within the volume of interest. For one measurement two consecutive laser pulses are fired within a very short time interval, and the radiation scattered by the particles in the illuminated area is recorded by a two-dimensional camera. The diameter of scattering particles usually is between 3 μm and 300 μm.

If the particles, scattering the light, are smaller than the wave-length of the light, Rayleigh-scattering occurs. Typical scattering particles in this case are molecules. There are two models to describe the interaction between the incoming light and the molecule, namely the model of the oscillating dipole and the simplified quantum mechanical model. For details reference is made to Bohren and Huffman (1983).

In Raman-spectroscopy a molecule initially absorbs a photon of the light hitting it of the wave-length λ_0. For visible light the energy of this photon is higher than what can be stored by rotation or vibration in the molecule, but often lower than the difference between the ground level and the first electronic state of the photon. Therefore the molecule is lifted up to a highly unstable, virtual level by absorbing the photon for a moment. The molecule afterwards immediately drops back to the stable energy level, if this new level is identical with the original level, Rayleigh-scattering will be observed. The principle for this change in energy is shown in Figure 22. If the new level is higher

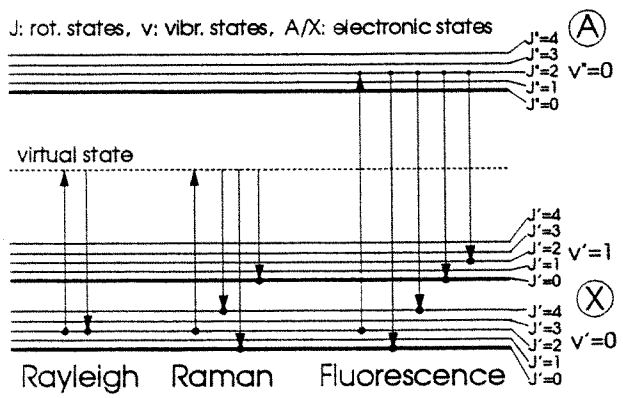

Fig. 22: Energy diagrams for Rayleigh, vibrational Raman-scattering and Laser-Induced-Fluorescence

or lower than the original level, the scattered light has a different frequency than the incidenting light. The shift in frequency is referred to as the Raman-shift and is proportional to the energy difference between the two molecular levels involved. One has to distinguish between rotational levels and vibrational levels of the molecule, and the difference between two rotational levels is much smaller than that of two vibrational levels. In Figure 22 the change in energy is shown for Rayleigh-scattering, for fluorescence and for Raman-scattering within 2 vibrational levels.

Since every species has its own energetical structure the observed frequency shifts can be related to certain molecules. Raman-scattering, therefore, provides an excellent possibility for detecting the concentration of several species in a gas-mixture of interest.

With Laser-Induced Fluorescence the molecule under consideration also absorbs one photon of the incoming laser-light. In this case, however, the energy of the photon must be equal to the energetic difference of two energy levels, the original level in the ground electronic state and a corresponding level in the first electronic state (see also Figure 22). Since the energy differences involved are discrete and specific for each species, the frequency of the laser has to be chosen in accordance with the molecule of interest. The states of the upper electronic levels are semi-stable with extremely short life-times and, therefore, soon after the transition to the upper state the excited molecule drops back to a stable energy level within the ground electronic state emitting a photon. In the most common case of a $X, v' = 0 \rightarrow A, v'' = 0$ (see Figure 22) excitation the mean part of fluorescence occurs at the same wave-length as the incoming light (e. g. excitation of OH with 308 nm with a XCl-Excimer laser). Therefore, it is sometimes difficult to distinguish between primary (incoming) radiation and the radiation by fluorescence in experiments with optical difficult accessibility. In competition to this Laser-Induced Fluorescence (LIF) a somewhat revised method was developed, the so-called Laser-Induced Predissociated Fluorescence (LIPF). Here the excitation transition is chosen such that predissociation at the upper state occurs in a high rate, and the wave-length of the fluorescing light is different from that of the incoming light for one and the same molecule. This method and also another method, the Laser Induced-Saturated Fluorescence (LISF), will not be discussed here. A good overview and detailed informations about the aforementioned fluorescence techniques can be obtained from the literature (e. g. Andresen, 1988 / 1990 / 1991, Hanson 1990).

4.1 Laser-Induced Fluorescence

Laser-Induced Fluorescence (LIF) and Laser-Induced Predissociated Fluorescence (LIPF) can be used to measure local concentrations in mass transfer processes or in chemical reactions. An arrangement of optical components for performing LIF or LIPF measurements is shown in Figure 23 exemplarily. A laser-beam must be used for electronically exciting of the molecules of interest. The wave-length of the laser must be adjusted to the substance, which should be investigated. For studying concentration fields in combustion processes the most active radical is of interest in this connection and this is, for example, the OH-radical in hydrogen combustion. For LIF-measurements the $X, v' = 0 \rightarrow A, v'' = 0$ excitation of the OH-radical has to be done with a wave-length of 308 nm, and the wave-length of the fluorescenting light is of the same value, therefore, one has the problem with LIF to separate carefully between the primary light of the exciting laser and the secondary light of the OH-Fluorescence. For LIPF-measurements the two-wave-lengths are different, for example, 248 nm for the exiting light and 290-304 nm for the fluorescenting light. Here it is easier to distinguish between primary and secondary light, however, the energy for producing LIPF is much higher than for LIF. To perform LIF, for example, an EXCIMER-laser filled with XeCl can be used, which has a bandwidth of 0,27 nm around the wave-length of 308 nm. To illuminate an area of approximately 50 cm^2 a pulse-energy of 150-200 mJ is needed. The pulse-duration of EXCIMER-lasers is around 20 ns.

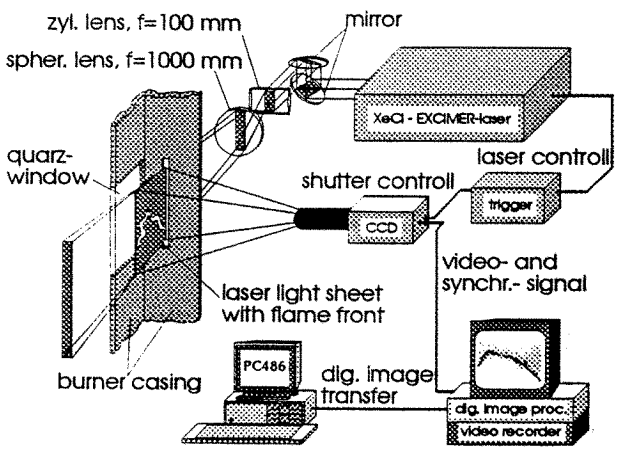

Fig. 23: Optical set-up for Laser-Induced Fluorescence

Figure 23 demonstrates how the laser-beam originating from the EXCIMER-laser is expanded and deformed into a thin light sheet with a height of approximately 5 cm and a thickness less than 0,7 mm. This

light sheet travels through a narrow quarz-window into the reaction zone where the fluorescence is produced in this thin layer. The fluorescence is observed and recorded in perpendicular direction to this light sheet with the aid of a CCD-camera, which is in this case intensified in the ultraviolet range of wavelengths. To get a good view of the fluorescenting area large quarz-windows have to be used, and the parts where no optical observations are intended have to be carefully painted with black colour for avoiding or damping light scattering in the reaction zone.

The video signal of the camera is processed in an image evaluating unit and transformed into pseudo-colour pictures. These pictures are recorded by a SVHS-video recorder working in an analog way. The timewise co-ordination of laser and camera is done via a triggering unit, which is synchronised by the video-camera.

For LIPF-measurements the same arrangement can be used, however, a laser must be available emitting light of shorter wave-length and higher energy-density. This can be done, for example, by using a Nd-YAG pumped Dye laser or a KrF-Excimer laser.

To demonstrate the capability of this optical method the influence of H_2 concentration on the stability of a flame-front travelling in a flowing H_2-air-mixture around an obstacle shall be briefly discussed in Figure 24. The flow velocity was 10-15 m/s and the obstacle - a rectangular plate - blocked approximately 2/3 of the cross-section of the channel. Going around the obstacle the flow produces Karman-vortices with intensive heat- and mass-transport, and the main reaction process is to be expected in this vortex-area. This is proven by the LIF recordings in Figure 24. Because of printing costs the varying OH-concentrations are presented there not in pseudo-colours, but in zones of different greyness.

At low H_2-content in the mixture - 9 vol % - the reaction is rather weak, and the flame can be even quenched in certain areas upstream of the obstacle. Increasing the H_2-content - 13 vol% - the quenching zones are drastically reduced and the contour of the flame in front of the obstacle is more steady. Finally at comparatively high H_2-content - 16,5 vol% - the flame covers a broad area in the channel. It has to be pointed out that none-steady flames were observed in Figure 24, which travel upward in the channel having a much higher velocity than the flow of the gas-mixture.

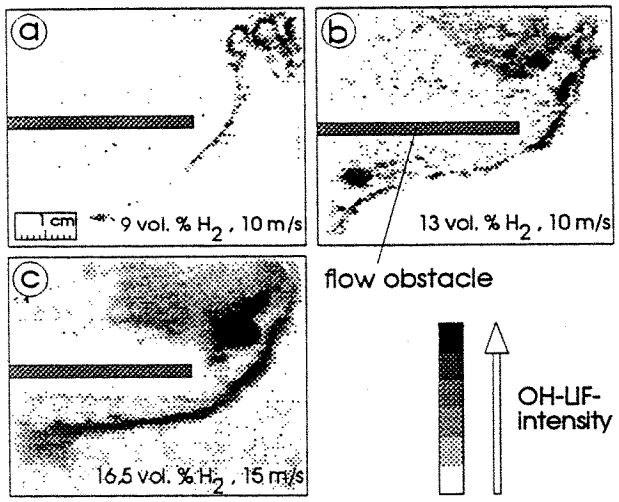

Fig. 24: OH-LIF records of an none-steady H_2-flame with an obstacle. a) 9 % H_2, flow velocity: 10 m/s, b) 13 % H_2, flow velocity: 10 m/s, c) 16.5 % H_2, flow velocity: 15 m/s (Ardey 1994)

4.2 Self-Fluorescence

It should be mentioned that with reacting gas-mixtures undergoing high enthalpy differences - for example in combustion-processes - also the method of the so-called self-fluorescence can be applied. Self-fluorescence can be observed, which is based on the fact that some of the molecules. appearing during the chemical reaction, already arise in an electronically excited state. A part of these excited particles radiate energy by spontaneous emission of photons in connection with a change in the energetic state of the molecule, which is refered to as chemo-luminiscence. The emitted energy is always equal to the difference of the two energetic states involved. Compared to laser-induced fluorescence the self-fluorescence has the disadvantage of low spectral signal intensities with the consequence of limited time and spatial resolution. On the other side, however, it is easy to handle and needs an only simple experimental set-up for obtaining insight into the overall structure and behaviour of fast reacting systems. An example of such a set-up is shown in Figure 25, which was used for investigating flames in supersonic flows (Haibel, 1992) (Haibel, 1993). Two intensified CCD-cameras were used to watch the flames from perpendicular directions in order to get some information about the three-dimensional structure of the flame. Each of these cameras was equipped with an interference filter, and each provides its signals to an image-processing and recording unit. Both cameras are synchronised by a timing device in order to record the images at the same instant of time. By reduc-

ing the exposure times down to a few μs the dynamic structure of the flame in a high-speed combustion chamber can be observed as Figure 26 demonstrates. There the OH-concentration in a hydrogen-diffusion-flame burning in a high-speed flow behind a step-shaped flame-holder is monitored from two directions. Exactly speaking, however, it is not the OH-concentration being present at the moment but the OH-production at this very short moment which produces the fluorescence.

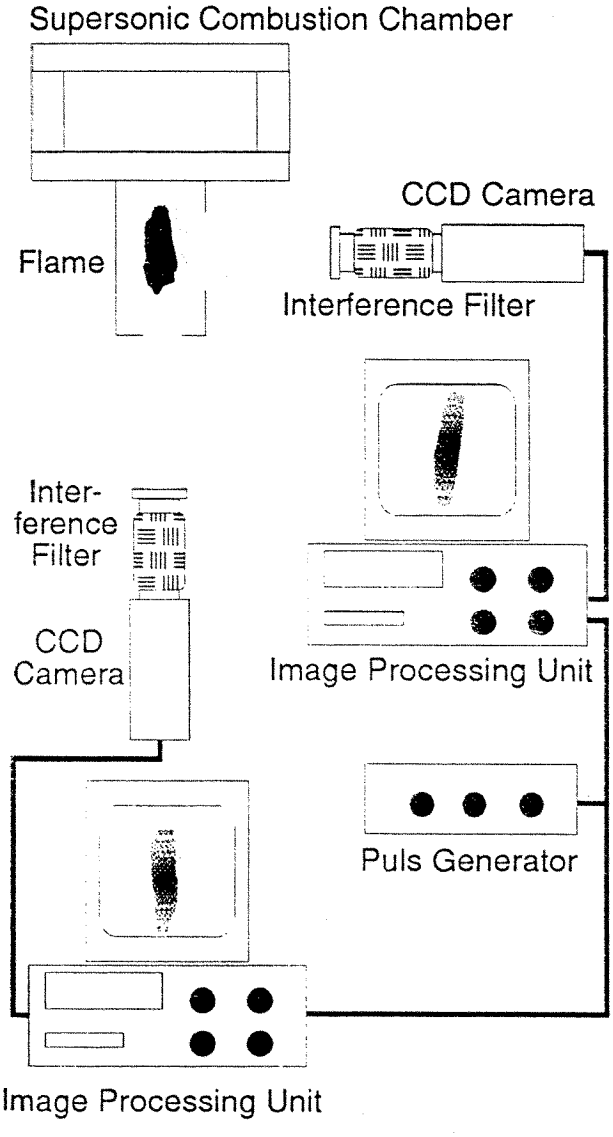

Fig. 25: Schematic set-up for self fluorescence investigations of high speed flames, observed from two directions (Haibel, 1993).

4.3 Raman-Spectroscopy

The theory of Raman-spectroscopy is well-described in the literature (for example, Long 1977, Alonso 1988 or Herzberg 1966) and shall not be discussed here. It is a non-intrusive method for measuring species-concentration, concentration ratios and temperatures of molecules. Raman-spectroscopy is applicable to any transparent medium regardless of its physical state. In heat and mass transfer the applications are usually concentrated to liquid or gaseous states while chemical and biological applications of them deal with solid samples.

Based on the Raman effect various methods for the measurement of temperature and concentration have been developed, some of them relying on special molecular resonance effects. The most widely used methods are Spontaneous Raman Scattering (SRS) or the Coherent Anti-Stokes Raman Scattering (CARS). The latter one provides light signals of higher intensity which is especially useful for gaseous applications. On the other hand the set-up and the evaluation of the results is for CARS much more complicated than for SRS.

The selection of the devices to spectrally resolve the scattered light depends on the property - concentration or temperature - to be investigated. Devices used for selecting the frequencies of the Raman-scattered light are interference filters or polychromators. If the intensity of the scattered light is to be measured at several different wave-lengths a set-up using filters becomes very complex regarding the alignment. The quantity of transmitted light is reduced by each surface to be penetrated. The polychromator is a more versatile choice but yields lower signal intensities to hit the light detection or recording device.

When Raman-spectroscopy is conducted using cw-lasers and photomultiplyer-tubes the necessary devices for data acquisition and control are not very complex. Pulsed lasers and diode arrays require more sophisticated equipment. For many applications complete systems including all necessary components for data acquisition and control are commercially available. They also include convenient routines and software for arithmetic routines.

An example for a set-up to measure species concentration and temperature with Raman-spectroscopy is shown in Figure 27 (Strube, 1993). Raman spectroscopy is a spotwise measurement technique and the laser-beam is therefore focused to a small spot, the diameter of which forms the measuring volume. The signal collection is usually arranged at a 90° an-

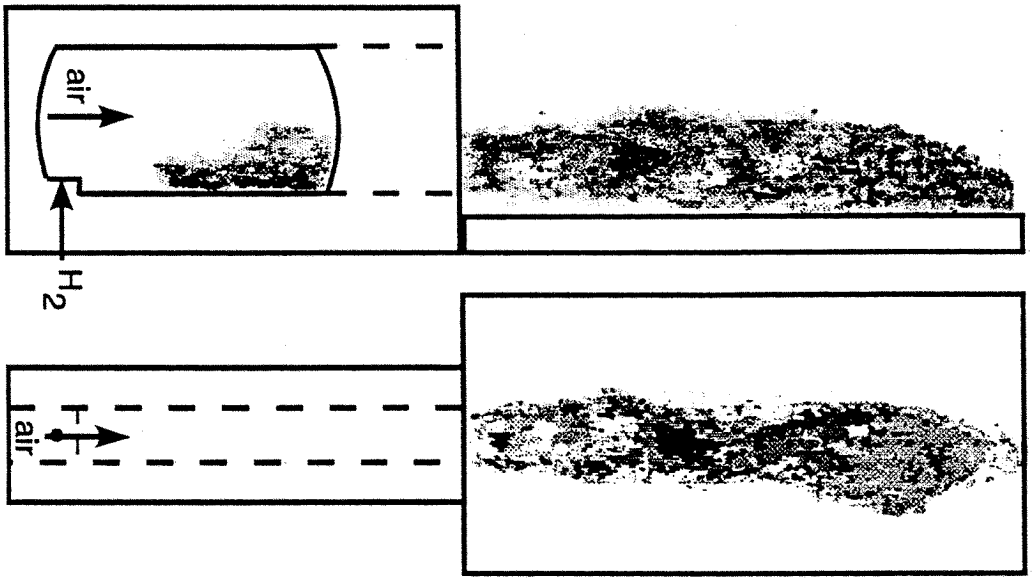

Fig. 26: False colour images of flames at a main Mach-number of 0.8. Both images show the flame at the same instant time at perpendicular directions of observations. The shutter speed was reduced to 50 μs (Haibel, 1993)

gle to the direction of the laser-beam. At this direction the signal intensity reaches a maximum and the size of the volume observed can be very well determined. If the vessel or channel enclosing the medium to be investigated allows the installation of a convex mirror opposite to the signal collecting lens the obtained signal intensity can be remarkably increased. In order to analyse the scattered intensities the collected light has to be resolved spectrally. This is accomplished either by diffraction units (for example polychromators) or selective filters. The intensity of the light at the selected wave-length is then converted into electronic signals, digitized and then numerically processed. Routines for data acquisition and for control are commercially available.

A very simple but - maybe - neat example of a result got with Raman-investigation is the comparison of room air with human breath. The upper spectrum in Figure 28 shows plane room air with a vapour content of 1,5% corresponding to a relative humidity of 60%. The lower spectrum is that of human breath blown through a small tube into the laser-spot. CO_2 appears at its two Raman active vibrational modes, its concentration is 8% corresponding to the decrease in O_2 concentration from 20% to 12%. The steam content increased from 1,5% to 3,5% corresponding to a relative humidity of 90%.

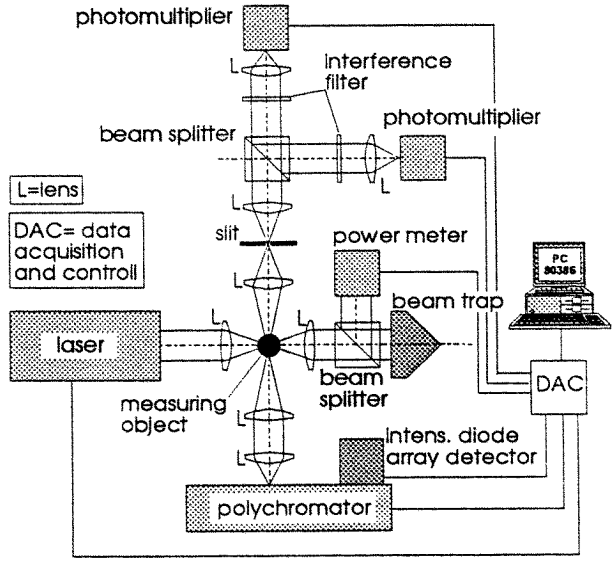

Fig. 27: Typical Raman set-up for point measurements. The two detection systems are only shown to demonstrate the different possibilities of arrangements, usually only one of the shown possibilites is used (Strube, 1993).

The temperature change can be measured from the difference in the height of the nitrogen peaks. Assuming that the nitrogen is not undergoing a chem-

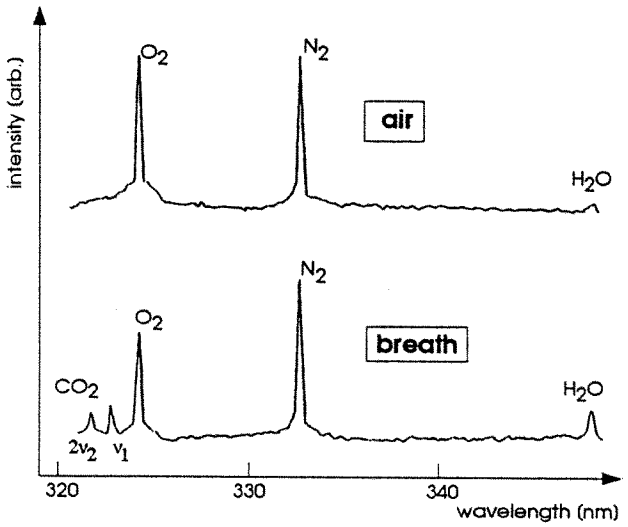

Fig. 28: Vibrational Raman spectra for room air and human breath as a simple, yet vivid example of the versatility of Raman-scattering

ical reaction the number of nitrogen molecules per unit of volume are proportional to the density of the nitrogen which in this case is only a function of the temperature. In the present example an evaluation of the nitrogen peaks gives a temperature rise from 21°C (incoming air) to 29°C in the breath.

If the temperature change is more pronounced, for example, during combustion, the difference in the peaks of none-reacting gases and by this the differences in the temperature levels can be much better seen in the Raman-spectra. This is very impressive, for example, by investigating hydrogen combustion, which is demonstrated in Figure 29. The experimental set-up was a stationary operated, closed tube type burner with a rectangular cross section. A metal grid was used to stabilise the flame. The premixed, unburnt gases with a hydrogen concentration of 12 volumetric % approach the grid upward with a velocity of 17 m/s. There is a separate turbulent flame stabilised behind each opening in the grid, and the burnt gases leave the flame area upward. Raman point measurements have been taken in a three-dimensional array. The concentration distributions are depicted for each species in the form of levels with various distances from the grid. The first spectrum is taken before the grid, no combustion has taken place, and so there is no steam present. The second spectrum is taken from the main reaction zone. Some of the hydrogen has reacted with parts of the oxygen to form steam as a product. All four species can be seen in the spectrum. The last spectrum is from a location above the reaction zone,

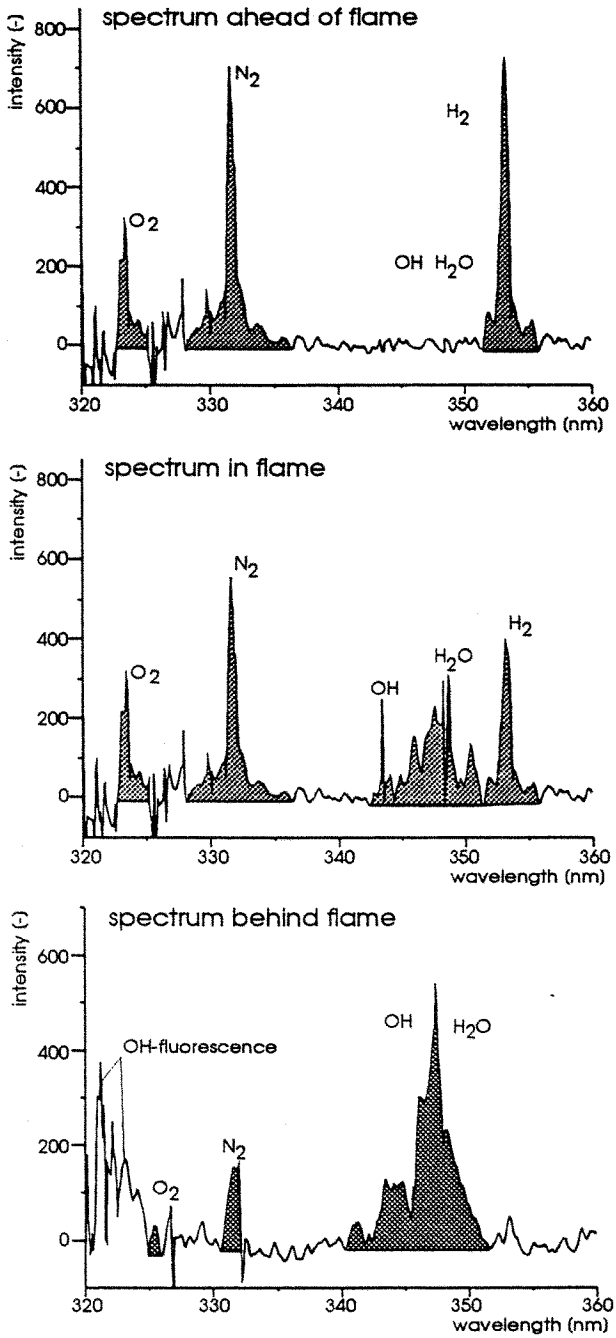

Fig. 29: Typical spectra from representative points in a burner. Top: unburnt mixture with 12 % H_2 in air. Middle: spectrum from the turbulent reaction zone. Bottom: completely burnt mixture (Strube, 1993).

where the under-stoichiometric combustion is complete. Only steam, nitrogen and the surplus oxygen are present there. Assuming the nitrogen behaves like an inert gas - or at least its oxidation is negligible - the temperature can be derived from the change of the integrated area under the nitrogen peak.

Finally Figure 30 demonstrates the very good local resolution of given concentration profiles. It shows as an example the nitrogen and hydrogen intensity distributions obtained from Raman measurements in a level of 17 mm above the grid briefly described before. The structure of the single flames above each opening of the grid is clearly visible. In order to show the change in relative hydrogen concentration due to the combustion the measured concentration of hydrogen has to be divided by the value for nitrogen. From the figure it can be seen that the spikes of nitrogen are larger in diameter than those of hydrogen indicating that the combustion mainly takes place at the conical surface of the flame.

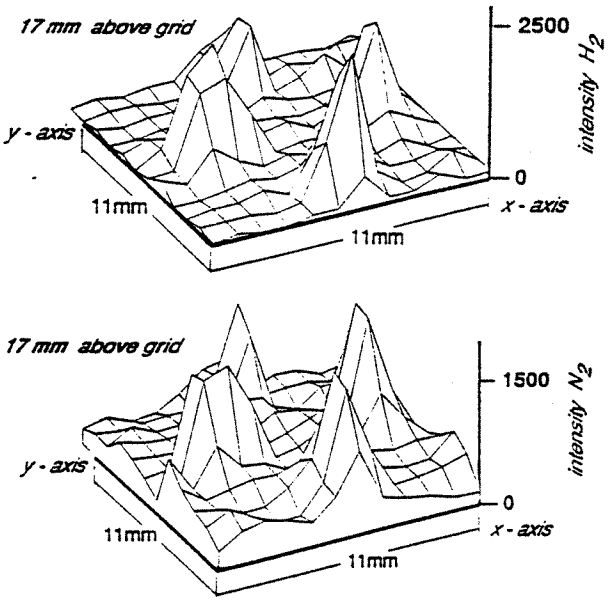

Fig. 30: Nitrogen and hydrogen intensity distributions obtained from measurements in level 17 mm above the grid.

5. CONCLUDING REMARKS

Optical techniques can be a very sensitive touchstone for physical modelling in developing computer codes. Sets of equations for computer codes in thermo- and fluiddynamics usually consist of two types of formulations, a first one derived from the conservation laws for mass, energy and momentum, and a second one which is mathematically modelling the transport processes like heat transport, turbulence or turbulent diffusion. For reliably predicting the heat transfer the velocity and the temperature field in the boundary layer must be known or a physically realistic and widely valid correlation for describing the turbulence must be available. For a better understanding of combustion processes it is necessary to know the local concentration and temperature just ahead of the flame and in the ignition zone. Visualized temperature-, concentration- or velocity-fields form an informative and realistic basis for developing theoretical models. For existing codes the grade of reliability and the extent of general validity can be checked or proved by optical techniques. On the other hand theoretical activities can and will create more demand for experiments based on optical techniques. Especially under transient conditions optical techniques provide great advantages, because they work non-invasive and inertialess. So modern electronics are of great advantage not only for physical modelling by numerical mathematics but also for data processing in experimental investigations.

Modern developments in industrial design provoke a great demand for a better understanding of physical and also of chemical - for example combustion - processes. A close co-operation between theoretical modelling and experimental verification can promote research and development. This demand together with the capabilities of modern electronic devices will enforce the revival of optical techniques.

6. LITERATURE

Alonso, M., Finn, E.J. (1988), Quantum Physics, Addison-Wesley

Andresen, P., Bath, A., Gröger, W., Lülf, H.W., Meijer, G., ter Meulen, J.J., 1988, Laser-Induced Fluorescence with tunable Laser as a possible method for instantaneous temperature field measurements at high pressures: Check with an athmospheric flame, Appl. Optics, 27:365, 1988

Andresen, P., Meijer, G., Schlüter, H., Voges, H., Koch, A., Hentschel, W., Oppermann, W., Rothe, E., (1990), Fluorescence imaging inside an internal combustion engine unsing tunable eximer lasers, Appl. Optics, 29:2392, June 1990

Andresen, P., Wolff, D., G., Schlüter, H., Voges, H., Koch, A., Hentschel, W., Oppermann, W., Rothe, E., (1990), Identification and imaging of OH (v"=0) and O_2 (v"=6 or 7) in an automobile engine using a tunable KrF eximer laser, Appl. Optics, 1991 submitted

Ardey, N., Beauvais, R., Mayinger, F., Strube, G., "Flame Propagation around a single Obstacle of instationary H_2-Air Flames", (German) Final Report BMFT 1500824, GRS 1994.

Bohren, C.F., Huffman D.R., (1983), Absorption and scattering by small particles, John Wiley and Sons, New York

Chávez, A., Mayinger, F. (1990)., Evaluation of pulsed laser holograms of spray droplets by applying image processing, 9th International Conference on Heat Transfer, 1990, p. 187.

Chávez, A., Mayinger, F. (1991).,Holografische Untersuchung an Einspritzstrahlen – Fluiddynamik und Wärmeübergang durch Kondensation, Diss. Techn. Univ. München, 1991.

Chávez, A., Mayinger, F. (1992)., Measurement of direct-contact condensation of pure saturated vapour on an injection spray by applying pulsed laser holography, Int. J. Heat Mass Transfer, Vol. 35 No. 3, pp 691-702, 1992.

Chen, Y. M., (1985)., Wärmeübergang an der Phasengrenze kondensierender Blasen, Diss. Techn. Universität München.

El-Wakil, M.M., Myers, G.E., Schilling, R.J. (1966)., An Interferometric Study of Mass Transfer from a Vertical Plate at Low Reynolds Numbers, J. of Heat Transfer, Vol. 88, p. 399.

Gonzales, R.C., Wintz, P. (1977), Digital image processing, Addison-Wesley, Massachussetts

Haberäcker, P. (1987), Digitale Bildverarbeitung, Grundlagen und Anwendungen, 2. Auflage, Hanser, München

Haibel, M., Mayinger, F., Turbulence enhanced mixing processes and stabilisation of sub- and supersonic H_2-air flames, Annual meeting of the DGLR, Bremen, Germany, Germany, 1992

Haibel, M., Mayinger, F., Strube, G. Application of non-intrusive diagnostic methods to sub- and supersonic H_2- air combustion, 3rd intl. Symposium on special topics in chemical propulsion: non-intrusive combustion diagnostics, Schwenningen, Germany, 1993

Hanson, R.K., Seitzmann, J.M., Paul, P.H. (1990), Planar fluorescence imaging of combustion gases, Applied Physics, Vol. B 50.

Hauf, W., Grigull, U. (1970)., Optical Methods in Heat Transfer, Advances in Heat Transfer, Vol. 6, p. 133.

Herzberg, G. (1966), Molecular spectra and molecular structure: Spectra of diatomic molecules, van Nostrand, New York.

Lighthart, G., Greon, C. (1982)., A Comparison of different autofocus algorithms, IEEE Transactions, Vol. XX, pp 597-604

Long, D.A.(1977), Raman spectroscopy, McGraw--Hill, London

Mayinger, F. (1994), Optical Measurements - Application and Potential, Springer Verlag Berlin.

Mayinger, F. (1991)., Optische Messverfahren in der Wärme- und Stoffübertragung, Ed. U. Grigull, Springer Verlag, Berlin.

Panknin, W., Mayinger, F. (1974)., Holography in Heat and Mass Transfer, 5th Int. Heat Transfer Conference, VI. 28, Tokio.

Panknin, W. (1977)., Eine holographische Zweiwellenlängen Interferometrie zur Messung überlagerter Temperatur- und Konzentrationsgrenzschichten, Diss. Universität Hannover.

Panknin, W., Mayinger, F. (1978)., Anwendung der holographischen Zweiwellenlängen Interferometrie zur Messung überlagerter Temperatur- und Konzentrationsgrenzschichten, Verfahrenstechnik, Vol. 12, No 9, pp 582-589.

Pavlidis, T. (1982), Algorithms for graphics and image processing, Springer Verlag, Berlin

Strube, G., Struktur und Brenngeschwindigkeit turbulenter, vorgemischter Wasserstoff-Flammen, Diss., Technische Universität München, 1993